Transgenerational effects of early life stress on the fecal microbiota in mice

Nize Otaru[1,2], Lola Kourouma[3, 4], Benoit Pugin[2], Florentin Constancias[2], Christian Braegger[1], Isabelle M. Mansuy[3, 4†*], Christophe Lacroix[2†*]

Affiliations:

[1] Nutrition Research Unit, University Children's Hospital Zürich, Zürich, Switzerland

[2] Laboratory of Food Biotechnology, Department of Health Sciences and Technology, ETH Zürich, Zürich, Switzerland

[3] Laboratory of Neuroepigenetics, Brain Research Institute, Medical Faculty of the University of Zurich, and Institute for Neuroscience, Department of Health Science and Technology of the ETH Zurich, Zurich, Switzerland

[4] Center for Neuroscience Zürich, ETH and University Zürich, Switzerland

† These authors jointly supervised this work

***Corresponding authors:**

Prof. Dr. Ing. Christophe Lacroix

E-mail: christophe.lacroix@hest.ethz.ch

Prof. Dr. Isabelle M. Mansuy

Email: mansuy@hifo.uzh.ch or imansuy@ethz.ch

Abstract

Stress in early life can affect the progeny and increase the risk to develop psychiatric and cardiometabolic diseases across generations. The cross-generational effects of early life stress have been modeled in mice and demonstrated to be associated with epigenetic factors in the germline. While stress is known to affect gut microbial features, whether its effects can persist across life and be passed to the progeny is not well defined. Here we show that early postnatal stress in mice shifts the fecal microbial composition (binary Jaccard index) throughout life. Further effects on fecal microbial composition and structure (weighted Jaccard index) are detected in the progeny across two generations. These effects are not accompanied by changes in bacterial metabolites and related predicted metabolic pathways in any generation. These results suggest that changes in the fecal microbial community induced by early life traumatic stress can be perpetuated from exposed parent to the offspring.

Introduction

It has long been established, that early life is a critical developmental window in which individuals are primed for life [1,2]. Traumatic stress in early life is one of the major causes of mental and physical diseases, particularly psychiatric disorders. These diseases often not only affect individuals directly exposed to early life stress but also sometimes their offspring [3–5]. Alterations in signaling pathways *via* the gut-brain axis have been suggested to contribute to the consequences of stress exposure [6]. Signaling *via* gut-brain axis is thought to occur by bacterially produced metabolites, such as short chain fatty acids (SCFAs) and γ-aminobutyric acid [7,8]. Since gastrointestinal tract maturation and the establishment of the gut microbiota occur in parallel with brain development [9], alterations in the gut microbiome may contribute to brain dysfunctions later in life. Experiments with germ free mice have indeed suggested the involvement of gut microbes in anxiety like behavior and behavioral despair induced by early life stress [10]. Early life stress has been shown to induce distinct gut microbial alterations in rodent models including the decrease of *Lactobacillaceae* species and increase in *Enterococcus* species. Though, observed changes are heterogenous and differ substantially between studies [11,12]. Similar observations exist in humans, though observed stress effects on the gut microbiota remain correlative and cannot be distinguished from confounding effects such as diet and lifestyle [11,13,14].

Previous research has mainly focused on changes in gut microbial composition rather than changes in function. In the few available human studies referring to gut microbial metabolic changes associated with early life stress, socioeconomic risk exposure explained a significant amount of the functional gut microbial diversity [15] and a decrease of four gut metabolites (i.e. glutamate gamma-methyl ester, 5-oxoproline, malate, and urate) was observed when comparing exposed with non-exposed individuals [13]. Given the effects of early life stress on brain functions and health in the progeny, it is conceivable that early life stress induced alterations in the gut

59 microbial community can also affect the offspring. Today, a potential intergenerational effect
60 of early life stress on the gut microbiota has not been carefully examined.

61 The mouse model of unpredictable maternal separation combined with unpredictable maternal
62 stress (MSUS) distinguishes itself from other rodent models of stress by applying
63 unpredictability as traumatic factor and by combining stress of mothers and of pups [16]. This
64 model has been extensively characterized and shown to induce behavioral, metabolic and
65 physiological alterations across generations [17,18]. Epigenetic factors in the germline have been
66 proposed as mediators of transmission and expression of phenotypes, and sperm RNA was
67 causally demonstrated to be a vehicle of transmission between exposed father and offspring and
68 grand-offspring [16,19,20]. Although, the MSUS paradigm has been shown to induce visceral
69 sensitivity [21], the effects of early life stress on the gut microbial community across generations
70 has not been evaluated before. Here, we show that postnatal traumatic stress modifies the fecal
71 microbial community in directly exposed mice but also in their offspring.

Results

Dynamics of fecal microbiota across life in healthy mice

To determine the dynamics of the fecal microbial community and its functionality across life in mice, the fecal microbiota from late postnatal to adult stages was analyzed.

Fecal microbial richness increases across life

Fecal microbial alpha diversity – the diversity within a community – was determined by assessing the richness and evenness of the community. Richness was defined as observed amplicon sequencing variants (ASVs) in a sample. Evenness was assessed with the Pielou's index, a measure indicating how evenly ASVs are distributed in a sample. Shannon diversity combines both richness and evenness in one function.

After weaning, microbial richness rapidly increased from median values of 226 (iqr: 54) to 348 (iqr: 57) observed ASVs in 22-day-old mice and 30-day-old mice, respectively (**Figure 1a**). Richness continued to increase across life span, although at a lower rate (log_2 fold-change), and reached a plateau in 15-week-old mice (**Figure 1**). In contrast, Pielou's and Shannon's index were the highest in 30-day-old mice but did not change thereafter (**Figure 1**).

Fecal microbial structure and composition changes across life

Beta diversity – diversity between communities – was evaluated using qualitative (binary Jaccard index) and quantitative (weighted Jaccard index) metrics. Fecal microbial composition was investigated *via* binary Jaccard index, and microbial structure was investigated *via* weighted Jaccard index.

Both, microbial composition and structure rapidly changed after weaning ($p < 0.01$ FDR-adjusted; $R^2 = 0.162$ and $R^2 = 0.180$) from 22-day-old to 30-day-old mice (**Figure 2**). Significant ($p < 0.05$, FDR-adjusted) differences in microbial composition and structure were

observed throughout life span, with lower effect size (determination coefficient; R^2) with increasing age (**Figure 2c**). In addition, 402 uniquely differently abundant ASVs ($p < 0.05$, FDR-adjusted) were detected across life (**Supplementary Figure 1**). In concurrence with changes observed in beta diversity, most differently abundant ASVs were observed comparing 22-day-old to older mice. Approximately half (176 ASVs) of differently abundant ASVs belonged to the family *Lachnospiraceae* (**Supplementary Figure 1**).

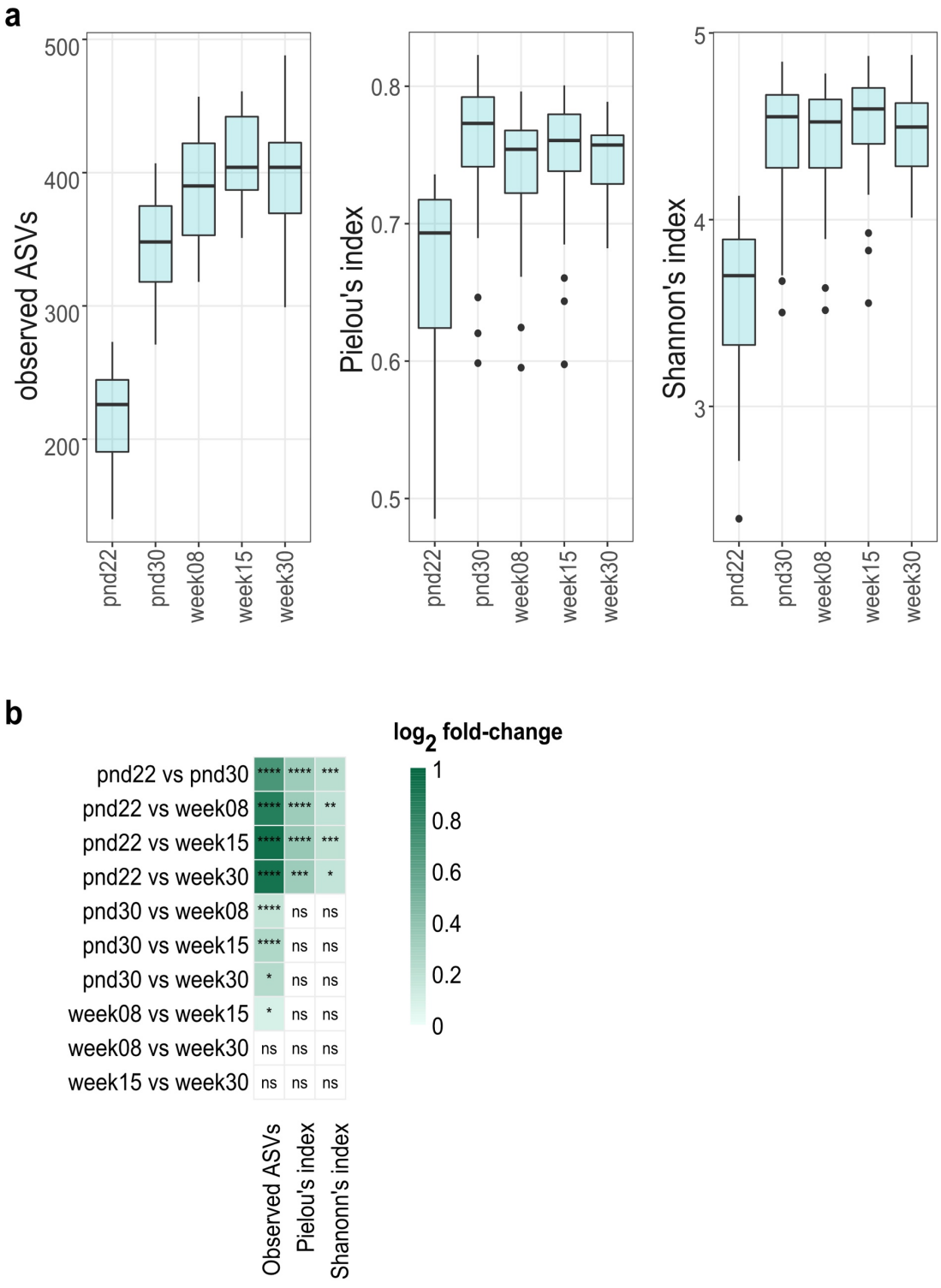

Figure 1: Effect of age on alpha diversity metrics of control mice fecal microbiota. (a) Fecal microbial richness (observed ASVs), evenness (Pielou's index), and Shannon-diversity across life. Boxplot with box elements showing upper and lower quantile and median. Whiskers extend from the hinge to ± 1.5 times the interquartile range or the highest/lowest value. Outliers are indicated as black points. (b) Log_2 fold-change in alpha diversity metrics per pairwise comparison of different ages. Significance was calculated using log_2 transformed metrics and generalized mixed effect models with FDR correction. ns: not significant; * $p < 0.05$; ** $p < 0.01$; *** $p < 0.001$; **** $p < 0.0001$

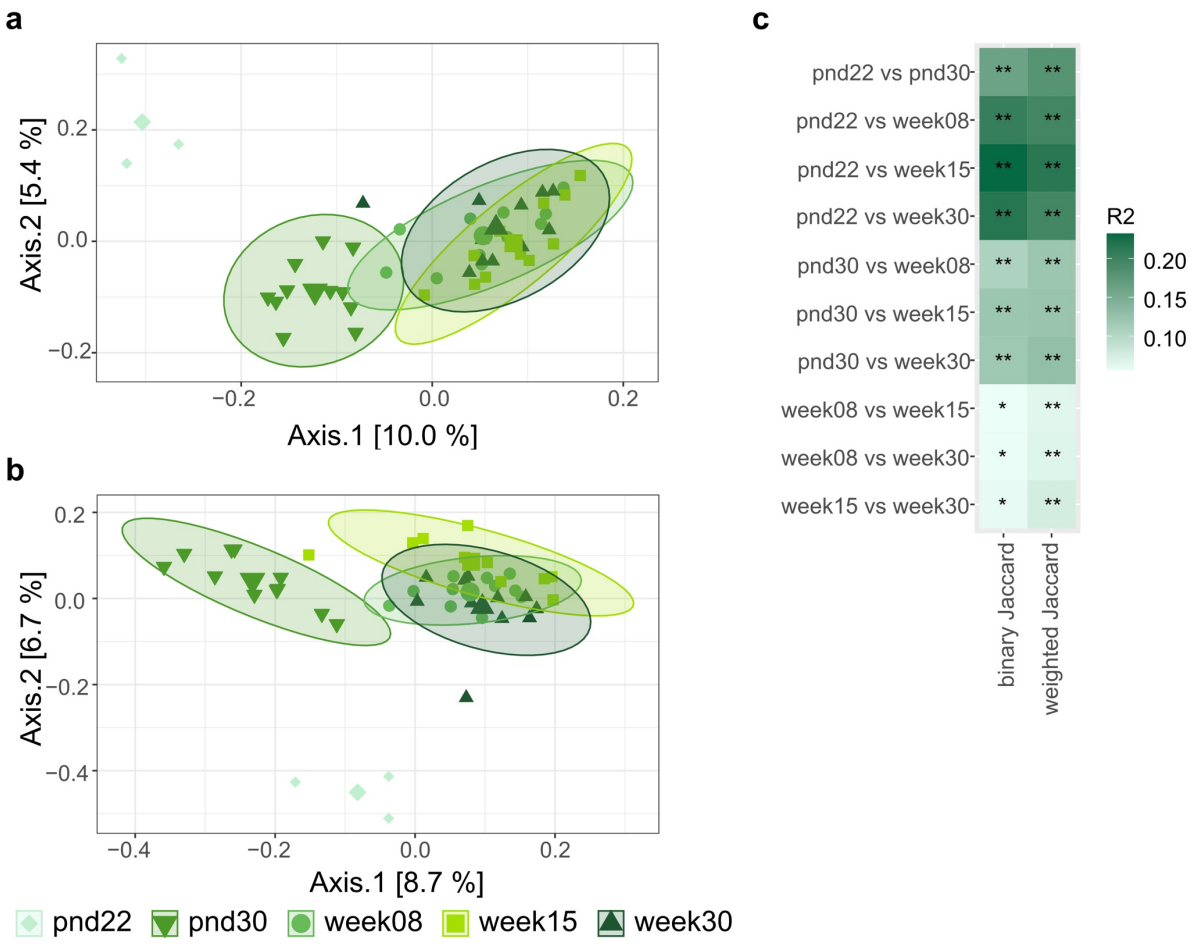

Figure 2: Effect of age on beta diversity metrics of control mice fecal microbiota. Visualization as principal correspondence analysis of (a) binary (microbial composition) and (b) weighted (microbial structure) Jaccard index. Individual symbols display aggregated microbiota per litter (pnd22) or cage (pnd30, week08, week15, and week30), large symbols display centroids, ellipses indicate 95% of confidence intervals. (c) Heatmap of R^2 for pairwise comparison of different ages. Significance was calculated using PERMANOVA including FDR correction. Pairwise comparison of different dispersions between ages are listed in **Supplementary Table 2**. pnd: postnatal day; * $p < 0.05$;** $p < 0.01$

Predicted fecal metabolic pathways change across life

To characterize the metabolic potential of the fecal microbiota throughout life, a functional prediction based on 16S rRNA amplicon sequences was performed. Accuracy of prediction was investigated *via* the abundance-weighted nearest sequenced taxon index (NSTI) which summarizes the extent to which ASVs in a sample are related to reference 16S rRNA genes. Low values indicate close relation, while large values indicate far relation to reference 16S rRNA gene.

Median of abundance-weighted average NSTI values was 0.18 (iqr: 0.03), indicating that on average prediction was performed based on taxa with 82% similarity. In total, 258 unique pathways were differentially abundant ($p < 0.05$, FDR-adjusted) at various time points (**Supplementary Figure 2**), suggesting functional changes in fecal bacterial community across life. In line with observations on beta diversity and differentially abundant ASVs, most differentially abundant pathways were identified comparing 22-day-old to older mice (**Supplementary Figure 2**).

Influence of the combination of behavioral testing and breeding on the fecal microbial community

To evaluate the effect of the temporal succession of behavioral testing and breeding, fecal microbiota of 30-week-old mice was examined in 2 different conditions: behavioral phenotyping conducted before breeding (GR1) or breeding conducted before behavioral testing (GR2). No significant differences in alpha diversity (richness, evenness, and Shannon's diversity) and beta diversity (binary and weighted Jaccard index) were observed between groups (**Supplementary Table 2**). However, 15 differentially abundant ASVs ($p < 0.05$, FDR-adjusted) were identified, all different in the range of 1.3 to 3.4 $\log_2$ fold-changes (**Figure 3a**). Relative abundance of these ASVs was generally low, with individual microbiota values ranging from 0% to 7.3% (**Supplementary Figure 3**).

In addition, 10 predicted metabolic pathways, related to carbohydrate and amino acid metabolism, were differentially abundant between groups ($p < 0.05$, FDR-adjusted), all different in the range of 0.4 to 1 $\log_2$ fold-changes (**Figure 3b**). In contrast, no differences in measured cecal bacterial organic acids, amino acids and amines were detected (**Supplementary Data; Supplementary Figure 4; Supplementary Figure 5**).

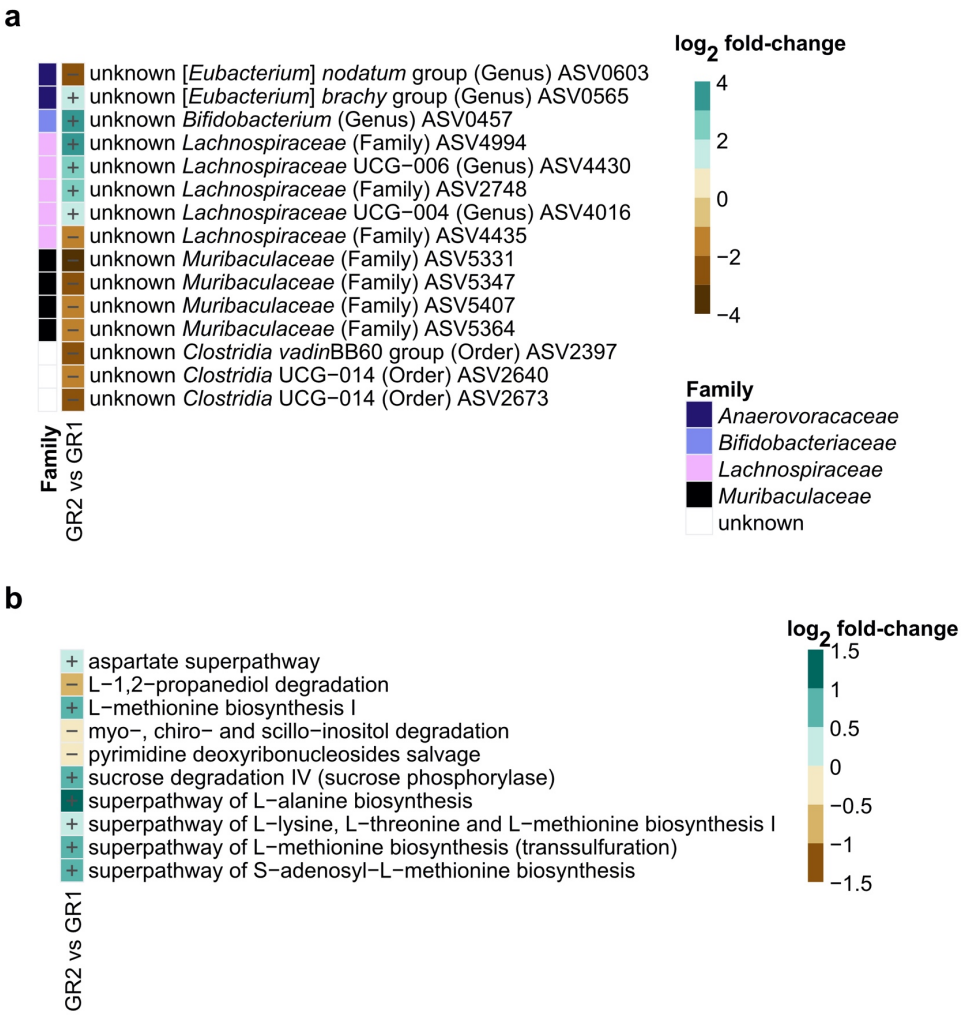

Figure 3: Effect of temporal succession of behavioral phenotyping and breeding on 30-week-old control mice fecal microbiota. Comparison of phenotyping group 2 (GR2; breeding before behavioral phenotyping) *versus* group 1 (GR1; behavioral phenotyping before breeding) microbiota. (a) Log_2 fold-change in specific ASVs significantly ($p < 0.05$, FDR-adjusted) decreased or increased in GR2 compared to GR1. Taxonomic information is indicated at family level. Relative abundances of individual ASVs are depicted in **Supplementary Figure 3**. (b) Log_2 fold-change in predicted fecal bacterial metabolic pathways significantly ($p < 0.05$, FDR-adjusted) decreased or increased in GR2 compared to GR1. Significance was calculated using $\log_2$ transformed abundance counts and generalized mixed effect models with FDR correction.

Early life stress induces a shift in fecal microbial community in directly exposed mice across life

To investigate if early life stress (MSUS paradigm) has a long-lasting effect on the fecal microbial community across life, the fecal microbiota was compared between F1 MSUS and control mice across the life span from 22 days till 30 weeks of age. In addition, animal weight was monitored in mice from 8 weeks to 30 weeks of age. Development of mice weight was not different between MSUS and controls ($p > 0.05$, FDR-adjusted) at different ages (**Supplementary Figure 6**).

Fecal microbial richness and evenness do not differ between F1 MSUS and controls across life

Different alpha diversity metrics were compared between F1 MSUS and control groups at different ages. No significant differences ($p > 0.05$, FDR-adjusted) in fecal microbial richness, evenness, and Shannon's diversity index between MSUS and controls were observed, with comparable median values for both groups at different ages (**Figure 4**).

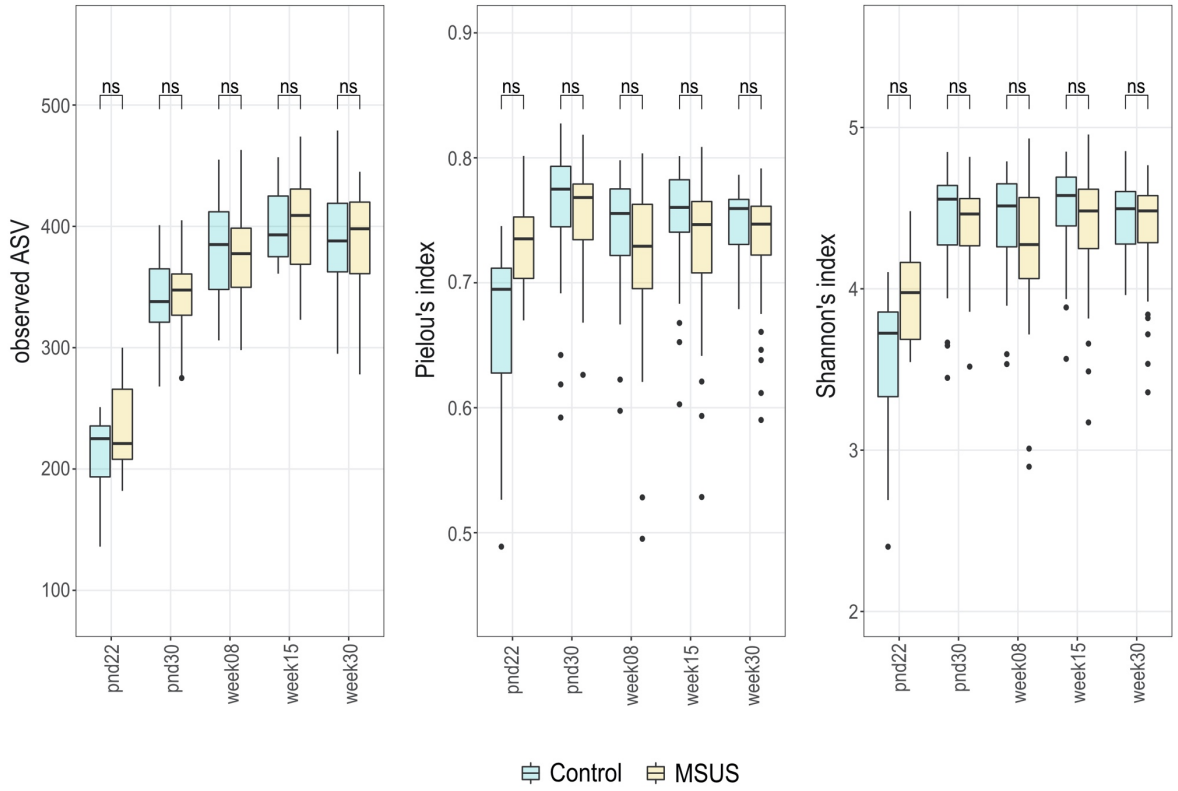

Figure 4: Comparison of different alpha diversity metrics between F1 MSUS and control fecal microbiota across life span. Comparison of richness (observed ASV), evenness (Pielou's index), and Shannon-diversity between MSUS and controls per time point. Boxplot with box elements showing upper and lower quantile and median. Whiskers extend from the hinge to ± 1.5 times the interquartile range or the highest/lowest value. Outliers are indicated as black points. Significance was calculated using $\log_2$ transformed metrics and generalized mixed effect models with FDR correction. pnd: postnatal day; ns: not significant

Fecal microbial composition differs between F1 MSUS and controls across life

Microbiota composition significantly differed between MSUS and controls in 30-day-old, 8-week-old, 15-week-old, and 30-week-old mice (binary Jaccard index; $p < 0.01$, FDR-adjusted; **Figure 5a-e; Figure 5k**). Microbiota structure significantly differed between MSUS and controls in 30-day-old mice (weighted Jaccard index; $p < 0.01$, FDR-adjusted**; Figure 5f-k**). Overall effect size was generally low with determination coefficients (R^2) ranging from 0.058 to 0.067 (**Figure 5k; Supplementary Table 3**).

Contrary to beta diversity, differentially abundant ASVs ($p < 0.05$, FDR-adjusted) were only detected for 8-week-old and 15-week-old mice, in the range of 0.98 to 3.06 $\log_2$ fold-changes (**Figure 6**). Yet, overall abundance of these ASVs was low, with individual microbiota values ranging from 0% to 1.9% (**Supplementary Figure 7; Supplementary Figure 8).** One ASV belonging to the Family *Ruminococcaceae* (ASV1948) was persistently decreased in MSUS compared to controls in both 8-week-old and 15-week-old mice.

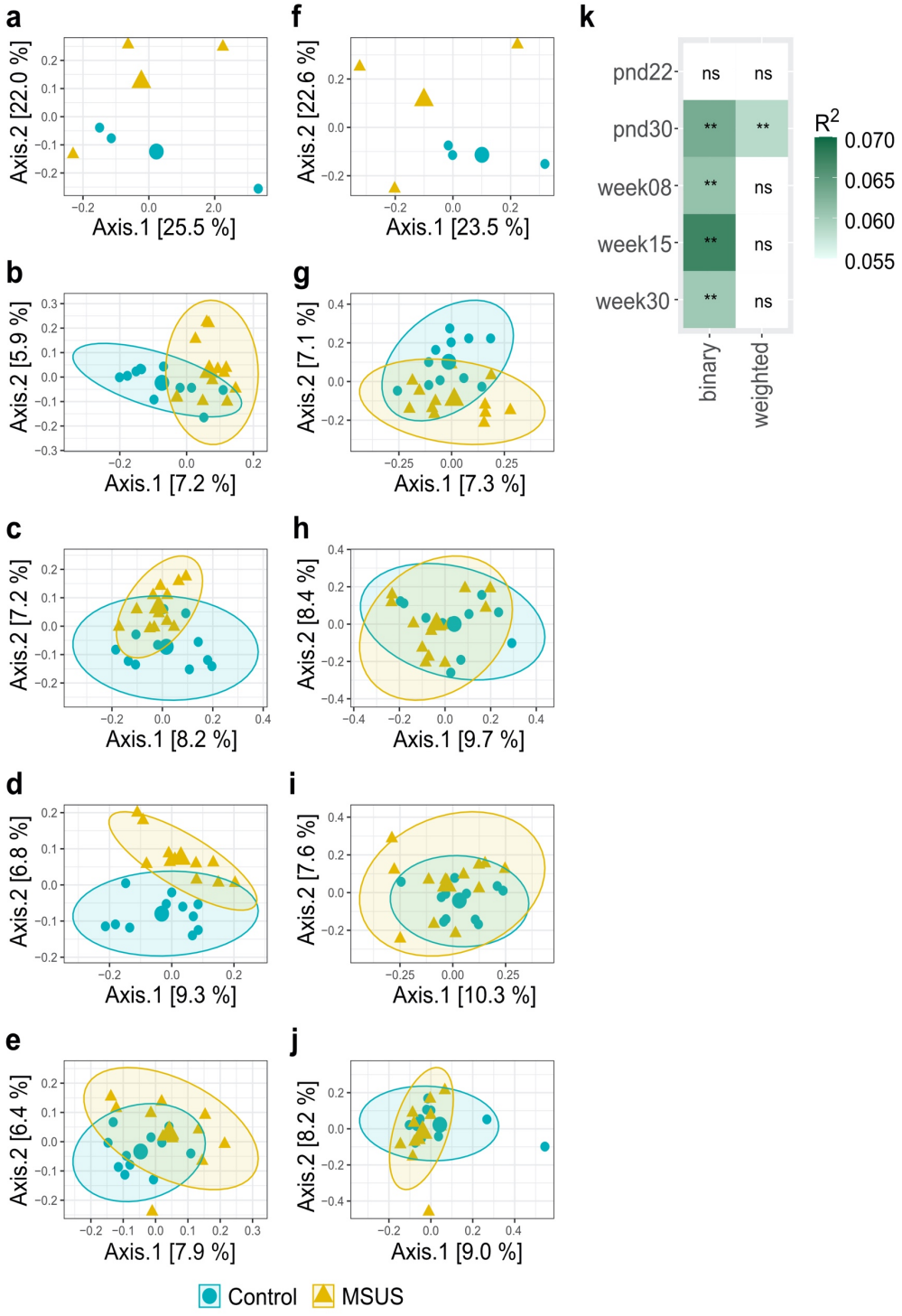

Figure 5: Effect of the MSUS paradigm on beta diversity metrics of fecal microbiota across life. Comparison of MSUS *versus* control mice is displayed. Visualization as principal correspondence analysis of (a-e) binary (microbial composition) and (f-j) weighted Jaccard index (microbial structure). (a,f) pnd22, (b,g) pnd30, (c,h) week08, (d,i) week15, and (e,j) week30 are depicted. Small symbols display aggregated microbiota per litter (pnd22) or cage (pnd30, week08, week15, and week30), large symbols display centroids, ellipses indicate 95% of confidence intervals. (k) Heatmap of R^2 for comparison between MSUS and control at different time points. Significance was calculated using PERMANOVA including FDR correction. Comparisons of different dispersions between MSUS and controls at different time points are listed in **Supplementary Table 3**. pnd: postnatal day; ns: not significant; ** $p < 0.01$

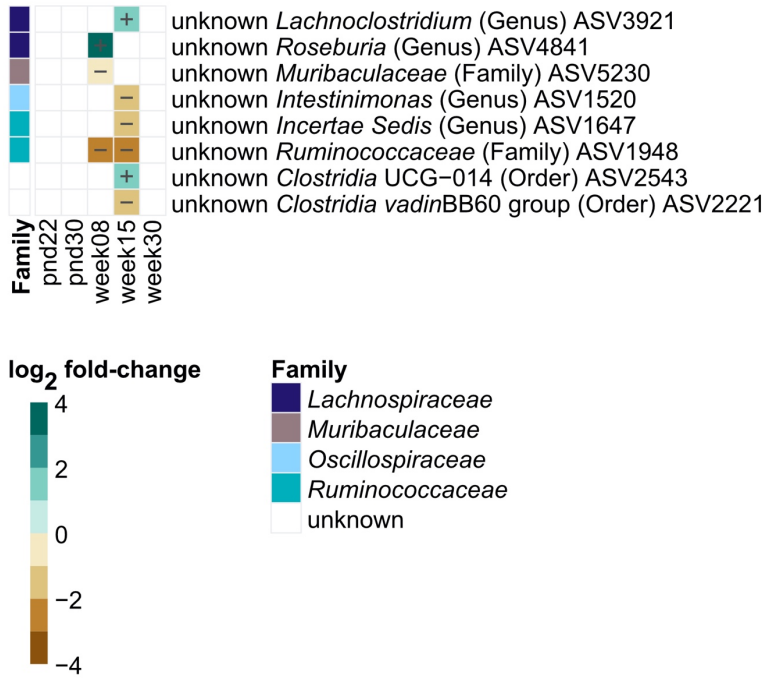

Figure 6: Log_2 fold-change in specific ASVs significantly ($p < 0.05$, FDR-adjusted) decreased or increased in F1 MSUS compared to controls over life. Taxonomic information is indicated at family level. Relative abundances of individual ASVs are depicted in **Supplementary Figure 7** and **Supplementary Figure 8**. Significance was calculated using log_2 transformed abundance counts and generalized mixed effect models with FDR correction.

Metabolic potential does not differ between F1 MSUS and controls across life

As a read out for the bacterial metabolic potential, metabolic pathways were predicted based on 16S rRNA amplicon sequences. Resulting median average-weighted NSTI value was 0.17 (iqr: 0.03), indicating that on average prediction was performed based on taxa with 83% similarity. In total, 287 unique bacterial metabolic pathways were predicted, with no significant ($p > 0.05$, FDR-adjusted) differences between MSUS and control mice for all tested ages. To further elaborate on metabolic potential, cecal bacterial organic acids, amino acids, and amines were evaluated for 30-week-old mice. Similarly, no significant ($p > 0.05$, FDR-adjusted) differences between MSUS and controls were observed, with comparable median values for both groups (**Supplementary Figure 9; Supplementary Figure 10**).

Early life stress shifts the trajectory of fecal microbial community across two generations

To investigate if early life stress in F1 alters the fecal microbial community in the progeny, fecal microbiota of mature adult MSUS and control mice (aged 28 or 30 weeks) were compared in the patriline (F2 and F3). It must be noted, that F3 mice were not direct offspring of investigated F2 mice, but of a subset of F2 mice which were not included in this study (**Figure 10**). Akin to results observed for F1 mice across life (**Supplementary Figure 5**), development of mice in terms of animal weight was consistent between MSUS and control mice in F2 and F3 (**Supplementary Figure 11**).

Fecal microbial composition and structure differ between MSUS and controls across two generations

To characterize the fecal microbial community, alpha diversity, beta diversity and differentially abundant ASVs were evaluated for each generation. Similar to results observed in F1 across life, fecal microbial richness, evenness, and Shannon's diversity did not significantly, differ between MSUS and controls for F2 and F3 (**Supplementary Figure 12**). As F1, F2, and F3 were sequenced in different runs (confounding factor), alpha diversity between generations was not directly compared.

Contrary to observations in mature adult F1 mice, where only an effect of the MSUS paradigm on microbiota composition (binary Jaccard index) was observed, both fecal microbial composition and structure significantly differed (weighted Jaccard index; $p < 0.05$, FDR-adjusted) between MSUS and controls in the patriline (F2 and F3; **Figure 7**). Effect size was highest in F3 with determination coefficients (R^2) of 0.130 and 0.099 for binary and weighted Jaccard index, respectively. This was approximately 2-fold higher when compared to F1 and F2 (**Figure 7g; Supplementary Table 4**). While no differently abundant ASVs were identified for mature adult F1 mice, in the patriline differently abundant ASVs ($p < 0.05$, FDR-adjusted), different in the range of 2.1 to 5.7 $\log_2$ fold-changes (**Figure 8**). Yet, overall abundance of these

ASVs was low, with individual microbiota values ranging from 0% to 2.7% (**Supplementary Figure 13; Supplementary Figure 14).** Half of observed uniquely differentially abundant ASVs, belonged to the family *Lachnospiraceae*. One ASV, belonging to the family *Muribaculaceae* (ASV5777), was persistently decreased in MSUS compared to controls in both F2 and F3 (**Figure 8**).

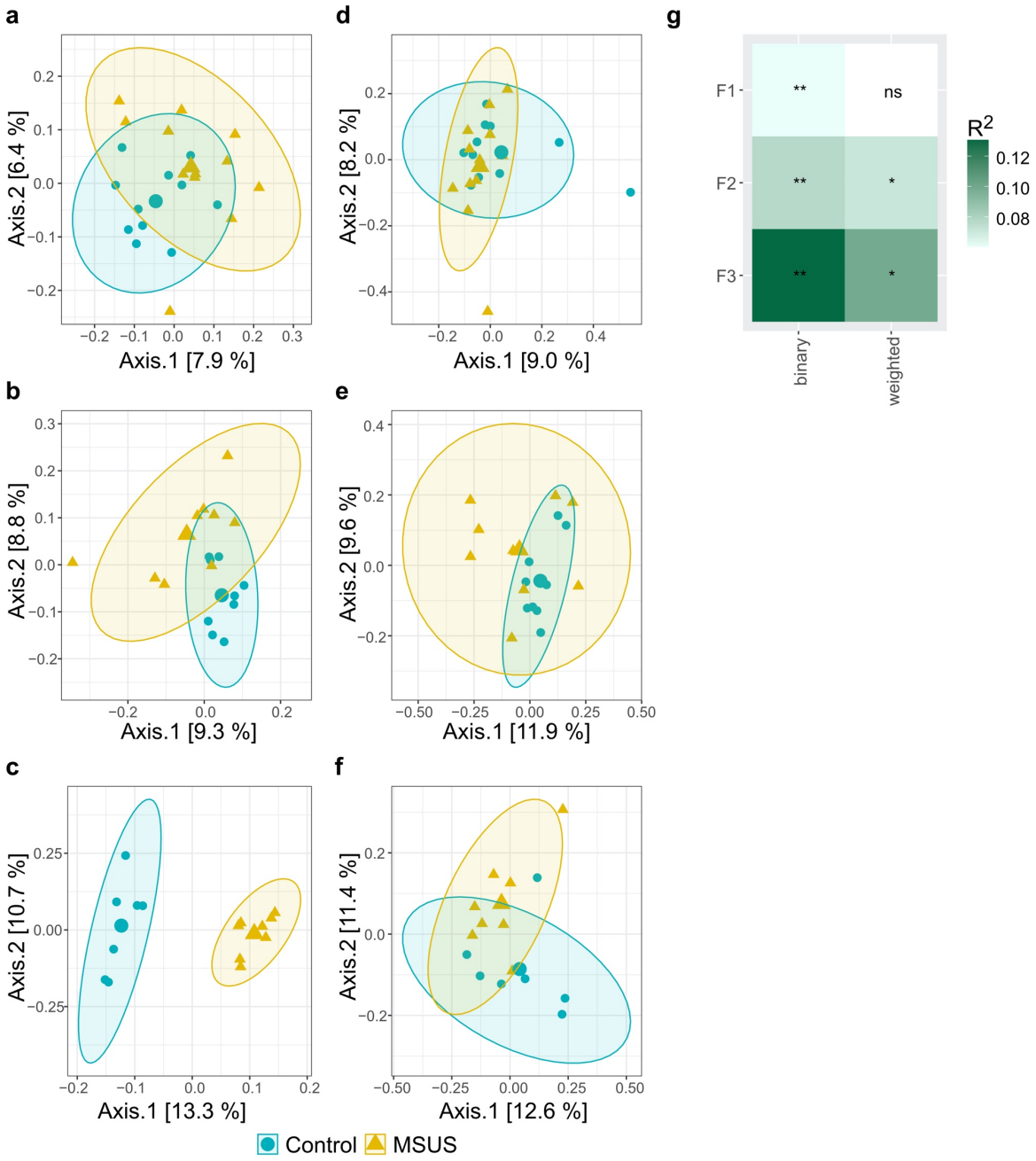

Figure 7: Effect of the MSUS paradigm on beta diversity metrics of F1, F2, and F3 mice microbiota. Comparison of MSUS *versus* control mice. Visualization as principal correspondence analysis of (a-c) binary (microbial composition) and (d-f) weighted Jaccard index (microbial structure). Small symbols display aggregated microbiota per cage, large symbols display centroids, and ellipses indicate 95% of confidence intervals. Microbial beta diversity of 30-week-old mice is depicted for (a,d) F1 and (c, f) F3, and microbial beta diversity of 28-week-old mice is depicted for (b, e) F2. (g) Heatmap of R^2 for comparison between MSUS and control across different generations. Significance was calculated using PERMANOVA including FDR correction. Comparisons of different dispersions between MSUS and controls at different time points are listed in **Supplementary Table 4**. ns: not significant; *$p < 0.05$; **$p < 0.01$

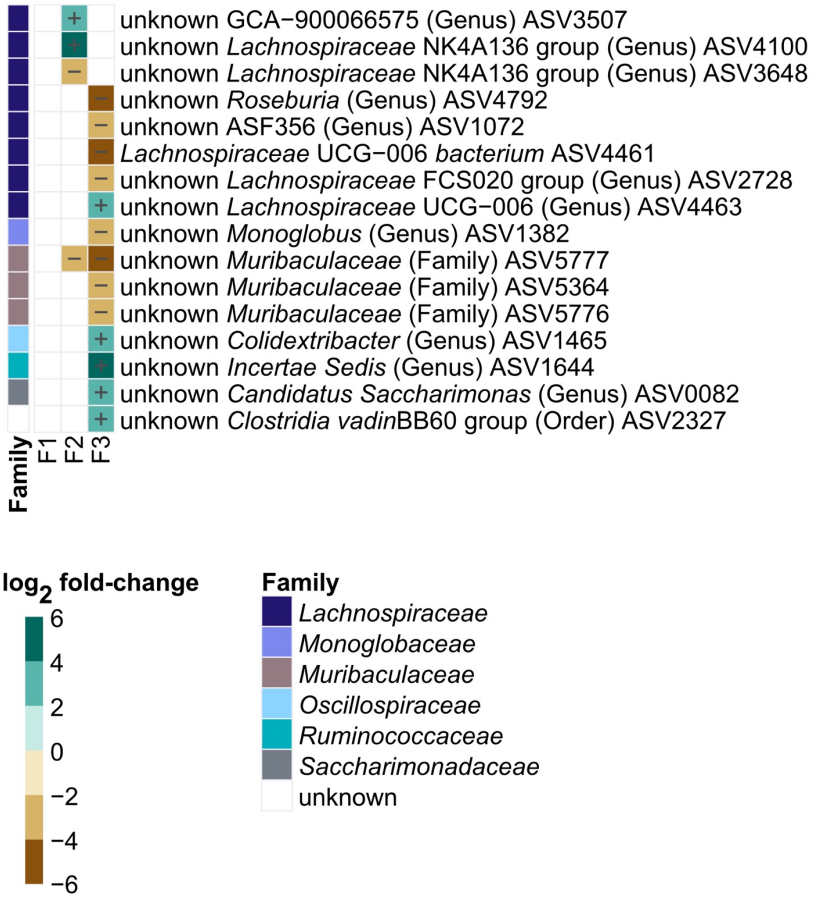

Figure 8: Log_2 fold-change in specific ASVs significantly ($p < 0.05$, FDR-adjusted) decreased or increased in MSUS compared to controls in F1, F2, and F3. Differentially abundant ASVs of 30-week-old mice are depicted for F1 and F3, and differentially abundant ASVs of 28-week-old mice are depicted for F2. Taxonomic information is indicated at family level. Relative abundances of individual ASVs are depicted in **Supplementary Figure 13** and **Supplementary Figure 14.** Significance was calculated using log_2 transformed abundance counts and generalized mixed effect models with FDR correction.

Metabolic potential does not differ between MSUS and controls across two generations

To investigate, if observed differences in fecal microbial community result in function changes, metabolic pathways were predicted based on 16S rRNA amplicon sequences. Resulting median abundance-weighted average NSTI value was 0.20 (iqr: 0.04), indicating that on average prediction was performed based on taxa with 80% similarity. In total, 286, 277, and 284 unique pathways were predicted for F1, F2, and F3, respectively. No significant difference ($p > 0.05$, FDR-adjusted) in pathway abundance between MSUS and controls were observed in all generations. Akin to observations in F1, no significant differences in cecal bacterial organic

acid, amino acid, and amine concentrations were detected in 28-week-old mice of F2 (**Supplementary Figure 15; Supplementary Figure 16**). Cecal bacterial metabolites were not evaluated in F3.

Fecal microbial community in offspring is not directly influenced by the father microbiota

To investigate, if observed differences in F2 MSUS *versus* controls stem from a transmission of fecal microbiota of MSUS-fathers to mothers and subsequently to offspring, beta diversity distances between pups and their parents, and between mating and non-mating pairs was evaluated. To minimize a potential effect of different phenotyping groups, father microbiota was evaluated before breeding or phenotyping, when mice were 16 weeks old.

Fecal microbial composition of 21-day-old pups was significantly (binary Jaccard index; $p < 0.0001$; FDR-adjusted) closer to mother microbiota than father microbiota for both MSUS and controls. Fecal microbial structure (weighted Jaccard index) was either as close to mother and father microbiota or significantly ($p < 0.05$; FDR-adjusted) closer to mother microbiota, for MSUS and control pups, respectively (**Figure 9a**). The older the pups (from 22-days-old to 16-weeks-old), the more similar the fecal microbial composition and structure got to parent microbiota, displayed by overall lower distances between microbiota. Microbial composition of 16-week-old pups remained significantly ($p < 0.001$; FDR-adjusted) closer to mothers than fathers. Microbial structure was either significantly ($p < 0.01$; FDR-adjusted) closer to father than mother microbiota, or as close to father and mother microbiota, for MSUS or control pups, respectively (**Figure 9a**). Mating and non-mating pairs showed no significant ($p > 0.05$; FDR-adjusted) difference in fecal microbial composition and structure. The temporal differences between sample collection and mating did not have an effect on observed distances, as indicated by absence of clustering according to phenotyping group (**Figure 9b**).

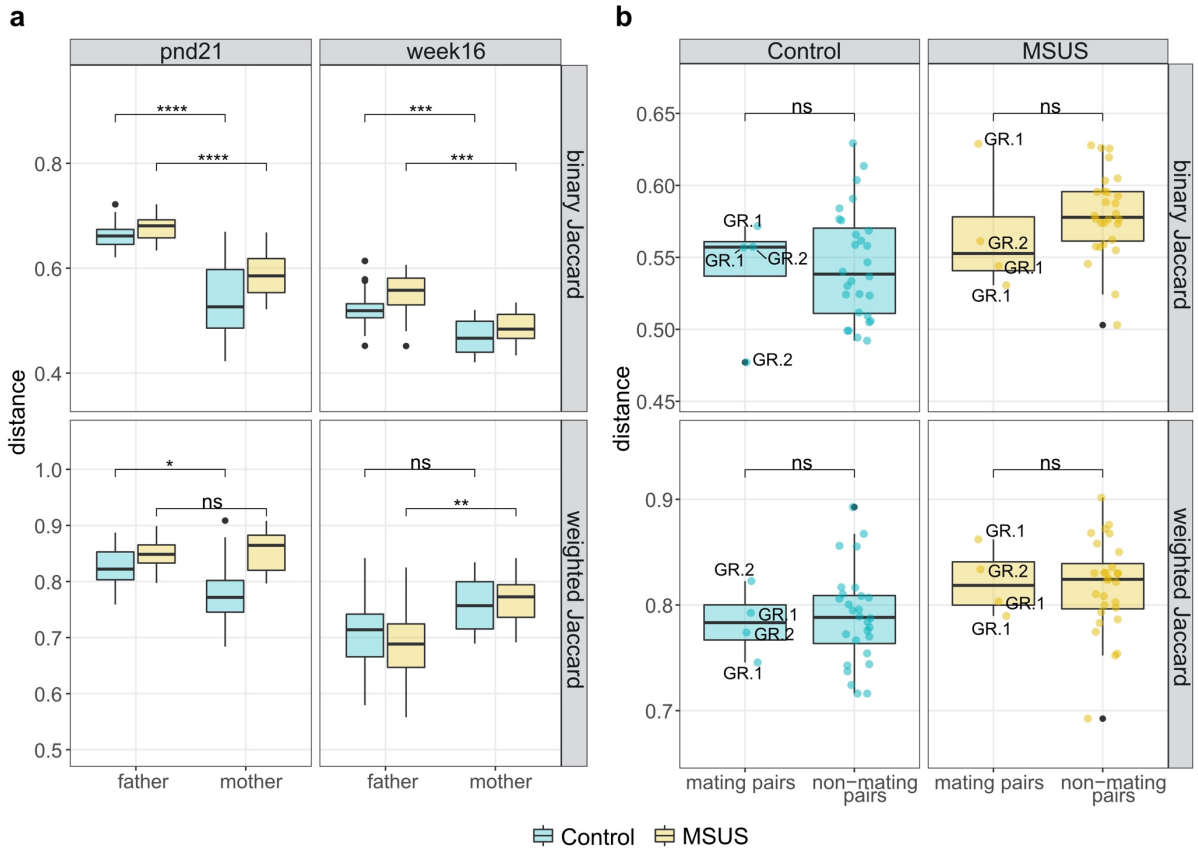

Figure 9: Comparison of different beta diversity metrics (binary and weighted Jaccard index) between F2 pups and their parents, and between mating pairs and non-mating pairs. (a) Distance between mother or father and respective pup microbiota at pup age pnd21 and week16. (b) Distance between mating pairs (n = 4) and non-mating pairs (n = 28). Boxplot with box elements showing upper and lower quantile and median. Whiskers extending from the hinge to +/- 1.5 times the interquartile range or the highest/lowest value. Colored points display individual distances and black points indicate outliers. Phenotyping group of fathers is indicated for mating pairs. Significance was calculated using Wilcoxon rank-sum test including FDR correction. pnd: postnatal day; ns: not significant; *$p < 0.05$; ** $p < 0.01$; *** $p < 0.001$; ****$p < 0.0001$; GR1: behavioral phenotyping before breeding; GR2: breeding before behavioral phenotyping

Discussion

Early life traumatic stress induces metabolic, and behavioral alterations across generations [17,18]. This study presents the first in-depth assessment of the effect of early life traumatic stress on the gut microbial community and metabolic functions in MSUS mice, while also addressing a transgenerational effect.

Early life stress has previously been shown to alter the fecal microbial community in studies focusing on a single time point after exposure [12,22,23]. Here we show in a longitudinal study that early life traumatic stress in mice results in significant changes in fecal microbial community composition (binary Jaccard index) persistent across life. However, significantly differentially abundant ASVs were largely different across life, with only one ASV being persistently decreased at two measured time points. ASVs belonging to the genus *Lachnoclostridium* were previously shown to be enriched in early life maternally separated mice [12], which we confirm here. Some previous studies found significant decreases in alpha diversity metrics upon early life stress exposure, while no significant difference in fecal microbial alpha diversity between early life stress exposed and non-exposed rodents were detected in the present and other studies [12,22,24,25]. These substantial differences between studies may result from different stress paradigms applied (i.e. maternal separation and/or early weaning or limited bedding and nesting), or from mouse husbandry factors, such as cage ventilation, chow, and bedding, which have previously been shown to substantially affect the gut microbial community [26–28]. Here we report no significant changes in fecal SCFAs, amines, amino acids, and predicted bacterial metabolic pathways between early life stress exposed and non-exposed mice across life. In contrary, in the only available study where the gut bacterial metabolome in mice was investigated upon early life stress exposure, a decrease in fecal lactate an increase in cholic acid in early life stressed mice compared to controls was observed [29].

Previous studies have shown the change of gut microbial features upon exposure to acute stress (e.g. heat, light, cold water, and restraint stress) in adult rodents [30–33]. Thus, it is conceivable that the applied stresses mothers are exposed to during the MSUS paradigm (i.e. restraint and acute swim stress) induce similar changes in the gut microbial community. These changes may then affect offspring, as it has been shown that disruption of mother's gut microbiota by antibiotics during nursing altered fecal microbial community and adaptive immunity in offspring [34]. Nevertheless, Kemp and colleagues (2021) suggest that gut microbial alterations due to early life stress occur independent of maternal microbiota inheritance.

The present study shows a transgenerational effect of early life traumatic stress induced changes on the fecal microbial community. Significant differences in fecal microbial composition (binary Jaccard index), structure (weighted Jaccard index), and relative abundances of several ASVs, between MSUS and control mice up to F3 were observed. We also show an increase in effect size with increasing number of generations (F1 to F3). However, only one ASV belonging to the family *Muribaculaceae* was persistently decreased in MSUS compared to controls in F2 and F3, suggesting different shifts in fecal bacterial community in MSUS mice of different generations.

Experiments with germ free mice have suggested a crucial involvement of gut microbes in anxiety like behavior and behavioral despair induced by early life stress [10]. Furthermore, after colonization of early life stressed germ-free mice distinct shifts in gut microbiota profiles were observed, which were not present in unstressed controls [10]. These observations suggest that early life stress exposure alters host factors, which modulate gut microbes, which then themselves signals back to the host exhibiting phenotypic changes. This notion could be present in F2 and F3 MSUS mice explaining observed gut microbial changes without directly experiencing early life traumatic stress beforehand. One candidate of communication between host and gut microbes independent of genetic background, might be non-coding RNAs. Long

non-coding RNA in gut tissue has been shown to substantially differ between conventionalized and different gnotobiotic mice [35]. In addition, small non-coding RNA such as microRNA are being released by intestinal epithelial cells and have been shown to be common in the gut lumen, where they may enter gut microbes and modulate gene expression and bacterial growth [36]. Conversely, gut microbes are thought to modulate intestinal epithelial microRNA expression most likely *via* excreted metabolites [37–40]. Thus, luminal microRNA has been suggested as a marker for host-microbiota homeostasis [41,42]. However, whether these non-coding RNAs are truly involved in the transgenerational effect on gut microbial community observed in the MSUS model remains highly speculative and would need to be addressed in future studies.

Though, the present study exhibits various strength, including relatively large sample size, monitoring of fecal microbial changes over time, and addressing the coprophagous nature of rodents (i.e. cage effect) it also has limitations. Fecal samples only serve as a proxy of the gut microbial community and functionality in the gastrointestinal tract. Akin to humans, pH and the gut microbial community varies along the gastrointestinal tract of mice and is thus considerably different from fecal samples [43]. In addition, a previous study has illustrated that the murine colon mucosa-associated and lumen microbial community are differentially affected by stress [44]. Thus, observations in the present study may not be directly extrapolated to all niches of the gastrointestinal tract. Biological relevance of observed microbial changes needs to be addressed in future studies. Direct cecal bacterial metabolite quantification was limited to one timepoint each in F1 and F2. In addition, bacterial metabolic pathway prediction *via* PICRUSt2 has several restrictions, especially for non-human samples. A recent study revealed that PICRUSt2 performs substantially worse for murine compared to human samples [45]. In addition, further bias is introduced due to the inability to detect strain specific functionality and the strong dependency on reference genomes [46]. The relatively large NSTI values observed in the present study, which are approximately 3.5-fold higher than values observed for the Human

Microbiome Project [46], suggest a lack of suitable sequences in the reference space. Together with the notion, that murine gut bacterial species are only in the process of being annotated and characterized [47], results need to be interpreted with caution. High-resolution techniques (i.e. metabolomics, shotgun metagenomics, or RNA sequencing) are warranted to address potential functional changes in gut microbiota between MSUS and controls over different generations.

In conclusion, the MSUS paradigm not only changes the fecal microbial community in directly exposed mice but also in their offspring. Further well-designed studies are warranted to validate and extend on present results, using high-resolution techniques and addressing host factors responsible for gut microbial modulation. Though, our distance based analyses (based on binary and weighted Jaccard index) suggested that the fecal microbial community in F2 mice were not directly linked to the father's microbiota. Further carefully designed experiments are warranted to entirely omit potential direct transmission of gut microbes from parents to offspring. For instance, assisted reproductive techniques such as artificial insemination could be used to avoid interactions between parents and eliminate related social confounds [48]. Previous research has shown that early life stress modulates the murine gut microbial community in a sex-dependent manner [49]. Whether changes in gut microbial features observed in the present study are also detectable in matrilines remains to be explored.

Material and Methods

Mouse husbandry and MSUS paradigm

Ethical approval was given by the Swiss cantonal regulations for animal experimentation under license numbers ZH057/15 and ZH083/18. All C57Bl/6J mice were kept in a temperature- and humidity-controlled facility under a reverse 12 h light/dark cycle with access to food and water *ad libitum*. Cage change took place once a week. First generation (F1) control and MSUS mice were obtained by breeding 3-month-old C57Bl/6J primiparous females with age-matched males. Pairs were kept in the same cage for one week. After birth, litters/dams were randomly assigned to control and MSUS groups. For MSUS group, dams were unpredictably separated from their pups for 3 h per day from postnatal day (pnd) 1 to 14, during which each mother was randomly exposed to restrain stress (20 min restraint in a tube) or acute swim stress (5 min in cold water, 18 °C). Controls were left undisturbed. At weaning (pnd 21) male pups were assigned to cages according to treatment and only including mice from different dams per cage, resulting in 3-5 mice per cage. After cage assignment, mice were tagged to allow for identification of individual mice throughout life. F1 control and MSUS mice were bred to naïve primiparous females to obtain second generation (F2) mice. Akin, F2 control and MSUS mice with no prior behavior testing were bred to naïve primiparous females to obtain third generation (F3) mice (**Figure 10**). Mice of F3 were not bred.

The present study was part of a bigger experiment, where behavior (i.e. risk-taking behavior and behavioral despair) was evaluated *via* elevated plus maze and forced swim test as described previously [19]. To evaluate effect of temporal succession of behavioral phenotyping and breeding, after fecal collection cages with 15-week-old (F1) and 16-week-old (F2) mice were randomly assigned to group 1 (GR1; behavioral phenotyping before breeding) or group 2 (GR2; breeding before behavioral phenotyping; **Figure 10**).

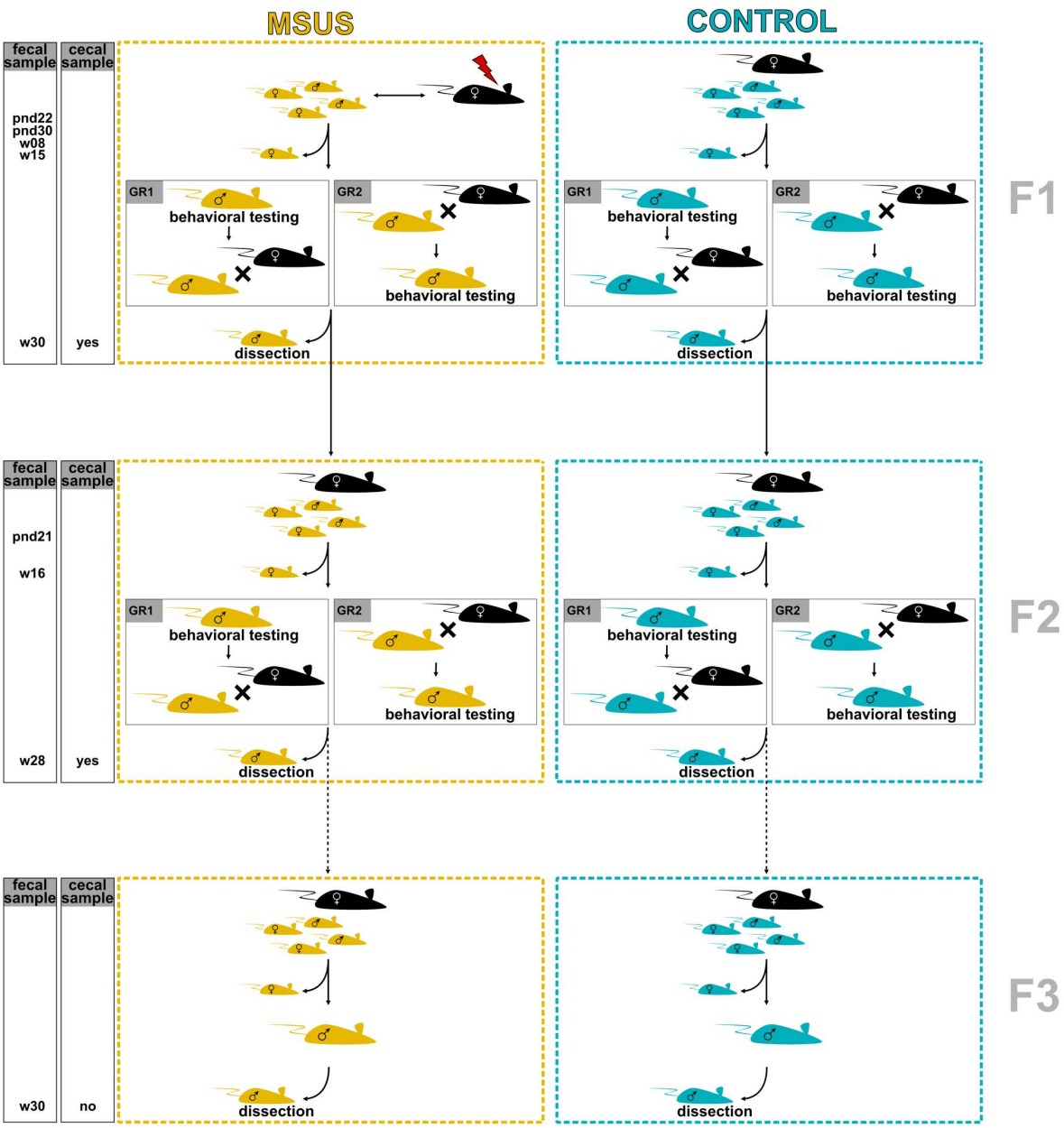

Figure 10: Experimental setup of mouse model. Setup and sample collection indicated across three generations. F3 mice are not direct offspring of displayed F2 mice (indicated by dashed line), but of a subset of F2 mice, which were not behaviourally phenotyped. Phenotyping group 1 (GR1): behavioral phenotyping before breeding. Phenotyping group 2 (GR2): breeding before behavioral phenotyping. pnd: postnatal day; w: week

Assessment of animal weight and collection of fecal and cecal samples

Animal weight was assessed for F1 mice at 8, 15, and 30 weeks of age, and for F2 and F3 mice at 28 and 30 weeks of age, respectively. For fecal sample collection, individual mice were placed on sterilized gloves worn by animal caretaker and let to defecate. At day of sacrifice,

fecal samples were directly collected from colon. For F1 mice fecal samples were collected for 22-day-old (after weaning), 30-day-old (after tagging), 8-week-old, 15-week-old, and 30-week-old (at day of sacrifice) mice (**Supplementary Table 4**). For F2 mice fecal samples were collected for 21-day-old (after weaning), 16-week-old, and 28-week-old (at day of sacrifice) mice (**Supplementary Table 4**). For both generations, cecal samples were collected at day of sacrifice. Mice were sacrificed approximately two months after behavioral testing. For F3, fecal samples were collected for 30-week-old (at day of sacrifice) mice only (**Supplementary Table 4**). Cecal samples of F2 dams (control: n = 4; MSUS: n= 6) were collected at day of sacrifice. All samples were frozen in liquid nitrogen immediately after collection and stored at -80 °C until analysis.

Cecal bacterial metabolite quantification

To determine bacterial metabolites in cecum content, samples were homogenized with 100 mM $HClO_4$ at a 1:3 ratio (w/v) followed by two centrifugation steps (6000 x g, 20 min and 14000 x g, 15 min, 4 °C). Resulting supernatant samples were stored at -80 °C until analysis. Samples were passed through a 0.2 µm nylon membrane prior to analysis with liquid chromatography as described previously [50]. Separation for organic acid quantification (i.e. SCFAs and intermediate metabolites) was conducted on a LaChrom HPLC-System (Merck-Hitachi, Japan) using a SecurityGuard Cartridges Carbo-H (4 × 3.0 mm; Phenomenex Inc., Torrance, CA, United States) connected to a Rezex ROA-Organic Acid H+ (300 × 7.8 mm; Phenomenex Inc.) column. Injection volume was 40 µl and elution was carried out at 40 °C under isocratic conditions, using 10 mM H_2SO_4 as eluent and a flow rate of 0.4 ml/min. Separated compounds were quantified using a refractive index detector L-2490 (Merck Hitachi). Raw data was analyzed using the EZChrom software (Agilent, Santa Clara, CA, United States).

For quantification of cecal amine, amino acid, and ammonia a pre-column derivatization was performed. In short, 100 µl of supernatant sample were mixed with 175 µl borate buffer (1 M H_3BO_3 adjusted to pH 9 with NaOH), 75 µl methanol, 4 µl internal standard (2 g/l L-2-aminoadipic acid, Sigma-Aldrich Chemie GmbH, Buchs, Switzerland), and 3.5 µl diethyl ethoxymethylenemalonate (VWR International AG, Dietikon, Switzerland) and incubated at room temperature in an ultrasonic bath for 45 min. Subsequently, samples were heated at 70 °C for 2 h to stop the derivatization reaction and passed through a 0.2 µm nylon membrane filter. Separation was carried out on an ACQUITY UPLC H-Class System (Waters Corp., Milford, MA, United States) using an ACQUITY BEH C18 column (1.7 µm particle size; 2.1 × 100 mm; Waters Corp.). Injection volume was 1 µl and elution was carried out at 40 °C with a flow rate of 0.46 ml/min, applying a gradient of 25 mM acetate buffer (pH 6.6), 100% methanol, and 100% acetonitrile as described previously [50]. Separated compounds were quantified using a diode array detector at 280 nm. Raw data was analyzed using the Empower 2 software (Waters Corp.).

Metabarcoding of bacterial community

DNA from fecal or cecal samples was extracted using the FastDNA Spin kit for soil (MP Biomedicals, Illkirch, France) according to manufacturer's instructions. The V4 16S rRNA gene region was amplified using the primers 515F (5′-GTGCCAGCMGCCGCGGTAA-3′) and 806R (5′-GGACTACHVGGGTWTCTAAT-3′). Subsequently, a tag-encoded MiSeq-based (Illumina, CA, USA) high throughput sequencing was performed, using an Illumina MiSeq System v2 including a flow cell with 2 × 250-bp paired-end Nextera chemistry supplemented with 10% (v/v) of PhiX as sequencing control. Samples from F1 were randomized in three different sequencing runs. Samples from F2 and F3 were sequenced in two separate runs.

All raw Illumina sequencing data was processed using the R package metabaRpipe [51]. In short, adaptors and V4 primers were removed using Atropos [52] and ASVs were constructed using the DADA2 pipeline [53]. Taxonomic assignment was performed using DADA2 formatted SILVA reference base (v138.1) with confidence threshold set to 50%. Raw Illumina sequences were deposited on the European Nucleotide Archive with the accession number PRJEB57336.

Statistics and reproducibility

Data and statistical analysis was carried out in R (v4.2.0) [54] using the packages, vegan (v2.5.7) [55], ape (v5.5) [56], ampvis2 (v2.7.9) [57], speedyseq (v0.5.3.9018) [58], Maaslin2 (v1.10.0) [59], and DivComAnalyses (v0.9) [60]. To calculate significance between two groups without confounders a Wilcoxon rank-sum test was performed. To calculate significance between groups and controlling for confounders generalized mixed effect models with false discovery rate (FDR) correction, using the Benjamini and Hochberg method, were applied. When applicable, cage, litter and sequencing run were treated as random effects while treatment (MSUS *versus* control), age, and phenotyping group were treated as fixed effects. Models were applied *via* Microbiome Multivariable Associations with Linear Models (MaAsLin 2) with minimal prevalence set to 0.25.

For alpha and beta diversity analyses sequences were rarified to equal sequencing depth. For comparison of alpha diversity indices generalized mixed effect models were applied *via* MaAsLin 2 using $\log_2$ transformed values. For beta diversity a linear model was fitted to various distance metrics. Homogeneity was investigated using a permutation test and effect of individual fixed effects was investigated *via* permutational multivariate analysis of variance (PERMANOVA). As random effects cannot be accounted for in PERMANOVA, an aggregation of samples per cage was performed prior to analysis to account for cage and litter effect (prior randomization of litter mates per cage).

Differential abundance testing was performed with MaAsLin 2 using $\log_2$ transformed relative abundance counts. Bacterial metabolic pathway prediction was performed using the Phylogenetic Investigation of Communities by Reconstruction of Unobserved States (PICRUSt2) software [46] and calculating MetaCyc pathway abundances [61]. MaAsLin2 with $\log_2$ transformed relative abundance counts was used to investigate differences between groups. Accuracy of PICRUSt2 prediction was investigated *via* the abundance-weighted NSTI. Differences in cecal metabolites were evaluated *via* MaAsLin2 with $\log_2$ transformed raw concentrations.

Significance level was set to $p \leq 0.05$. Median values are stated including interquartile range (iqr) in brackets. In boxplots, outliers are indicated and defined as values greater than 1.5 times the iqr over the 75th percentile and values smaller than 1.5 iqr under the 25th percentile. Data visualization was performed in R using ggplot2 (v3.3.5) [62] and ComplexHeatmap (v2.13.1) [63].

References

1. Nelson, C. A., Zeanah, C. H. & Fox, N. A. How early experience shapes human development: the case of psychosocial deprivation. *Neural Plast* **2019**, 1–12 (2019).
2. Ratsika, A., Codagnone, M. C., O'Mahony, S., Stanton, C. & Cryan, J. F. Priming for life: early life nutrition and the microbiota-gut-brain axis. *Nutrients* **13**, 423 (2021).
3. Gershon, A., Sudheimer, K., Tirouvanziam, R., Williams, L. M. & O'Hara, R. The long-term impact of early adversity on late-life psychiatric disorders. *Curr Psychiatry Rep* **15**, (2013).
4. McEwen, B. S. Understanding the potency of stressful early life experiences on brain and body function. *Metabolism* **57**, 11–15 (2008).
5. Bowers, M. E. & Yehuda, R. Intergenerational Transmission of Stress in Humans. *Neuropsychopharmacol* **41**, 232–244 (2016).
6. Clarke, G., O'Mahony, S. M., Dinan, T. G. & Cryan, J. F. Priming for health: gut microbiota acquired in early life regulates physiology, brain and behaviour. *Acta Paediatr* **103**, 812–819 (2014).
7. O'Riordan, K. J. *et al.* Short chain fatty acids: Microbial metabolites for gut-brain axis signalling. *Mol Cell Endocrinol* **546**, 111572 (2022).
8. Mazzoli, R. & Pessione, E. The neuro-endocrinological role of microbial glutamate and GABA signaling. *Front Microbiol* **7**, 1–17 (2016).
9. Jena, A. *et al.* Gut-brain axis in the early postnatal years of life: a developmental perspective. *Front Integr Neurosci* **14**, 1–18 (2020).
10. De Palma, G. *et al.* Microbiota and host determinants of behavioural phenotype in maternally separated mice. *Nat Commun* **6**, 7735 (2015).
11. Hantsoo, L. & Zemel, B. S. Stress gets into the belly: early life stress and the gut microbiome. *Behav Brain Res* **414**, 113474 (2021).
12. Kemp, K. M., Colson, J., Lorenz, R. G., Maynard, C. L. & Pollock, J. S. Early life stress in mice alters gut microbiota independent of maternal microbiota inheritance. *Am J Physiol Integr Comp Physiol* **320**, R663–R674 (2021).
13. Coley, E. J. L. *et al.* Early life adversity predicts brain-gut alterations associated with increased stress and mood. *Neurobiol Stress* **15**, 100348 (2021).
14. Callaghan, B. L. *et al.* Mind and gut: associations between mood and gastrointestinal distress in children exposed to adversity. *Dev Psychopathol* **32**, 309–328 (2020).
15. Flannery, J. E. *et al.* Gut feelings begin in childhood: the gut metagenome correlates with early environment, caregiving, and behavior. *mBio* **11**, e02780-19 (2020).
16. Franklin, T. B. *et al.* Epigenetic transmission of the impact of early stress across generations. *Biol Psychiatry* **68**, 408–415 (2010).
17. van Steenwyk, G. *et al.* Involvement of circulating factors in the transmission of paternal experiences through the germline. *EMBO J* **39**, e104579 (2020).

18. van Steenwyk, G., Roszkowski, M., Manuella, F., Franklin, T. B. & Mansuy, I. M. Transgenerational inheritance of behavioral and metabolic effects of paternal exposure to traumatic stress in early postnatal life: evidence in the 4th generation. *Environ Epigenet* **4**, dvy023 (2018).

19. Gapp, K. *et al.* Alterations in sperm long RNA contribute to the epigenetic inheritance of the effects of postnatal trauma. *Mol Psychiatry* **25**, 2162–2174 (2020).

20. Gapp, K. *et al.* Implication of sperm RNAs in transgenerational inheritance of the effects of early trauma in mice. *Nat Neurosci* **17**, 667–669 (2014).

21. Moloney, R. D. *et al.* Early-life stress induces visceral hypersensitivity in mice. *Neurosci Lett* **512**, 99–102 (2012).

22. Reemst, K. *et al.* The role of the gut microbiota in the effects of early-life stress and dietary fatty acids on later-life central and metabolic outcomes in mice. *mSystems* **7**, e0018022 (2022).

23. Usui, N., Matsuzaki, H. & Shimada, S. Characterization of early life stress-affected gut microbiota. *Brain Sci* **11**, 913 (2021).

24. Karen, C., Shyu, D. J. H. & Rajan, K. E. *Lactobacillus paracasei* supplementation prevents early life stress-induced anxiety and depressive-like behavior in maternal separation model-possible involvement of microbiota-gut-brain axis in differential regulation of microRNA124a/132 and glutamate Rec. *Front Neurosci* **15**, 719933 (2021).

25. Enqi, W., Jingzhu, S., Lingpeng, P. & Yaqin, L. Comparison of the gut microbiota disturbance in rat models of irritable bowel syndrome induced by maternal separation and multiple early-life adversity. *Front Cell Infect Microbiol* **10**, 581974 (2021).

26. Bidot, W. A., Ericsson, A. C. & Franklin, C. L. Effects of water decontamination methods and bedding material on the gut microbiota. *PLoS One* **13**, e0198305 (2018).

27. Ericsson, A. C. *et al.* The influence of caging, bedding, and diet on the composition of the microbiota in different regions of the mouse gut. *Sci Rep* **8**, 4065 (2018).

28. Franklin, C. L. & Ericsson, A. C. Microbiota and reproducibility of rodent models. *Lab Anim (NY)* **46**, 114–122 (2017).

29. Riba, A. *et al.* Early life stress in mice is a suitable model for irritable bowel syndrome but does not predispose to colitis nor increase susceptibility to enteric infections. *Brain Behav Immun* **73**, 403–415 (2018).

30. Qu, Q. *et al.* Effects of heat stress on gut microbiome in rats. *Indian J Microbiol* **61**, 338–347 (2021).

31. Zhang, Y. *et al.* Acute cold water-immersion restraint stress induces intestinal injury and reduces the diversity of gut microbiota in mice. *Front Cell Infect Microbiol* **11**, 706849 (2021).

32. Kim, Y.-M. *et al.* Light-stress influences the composition of the murine gut microbiome, memory function, and plasma metabolome. *Front Mol Biosci* **6**, 108 (2019).

33. Bassett, S. A. *et al.* Metabolome and microbiome profiling of a stress-sensitive rat model of gut-brain axis dysfunction. *Sci Rep* **9**, 14026 (2019).

34. Nyangahu, D. D. *et al.* Disruption of maternal gut microbiota during gestation alters offspring microbiota and immunity. *Microbiome* **6**, 124 (2018).

35. Liang, L., Ai, L., Qian, J., Fang, J.-Y. & Xu, J. Long noncoding RNA expression profiles in gut tissues constitute molecular signatures that reflect the types of microbes. *Sci Rep* **5**, 11763 (2015).

36. Liu, S. *et al.* The host shapes the gut microbiota via fecal microRNA. *Cell Host Microbe* **19**, 32–43 (2016).

37. Nakata, K. *et al.* Commensal microbiota-induced microRNA modulates intestinal epithelial permeability through the small GTPase ARF4. *J Biol Chem* **292**, 15426–15433 (2017).

38. Williams, M. R., Stedtfeld, R. D., Tiedje, J. M. & Hashsham, S. A. MicroRNAs-based inter-domain communication between the host and members of the gut microbiome. *Front Microbiol* **8**, 1896 (2017).

39. Zhao, Y. *et al.* Probiotics and microRNA: their roles in the host–microbe interactions. *Front Microbiol* **11**, 604462 (2021).

40. Hu, S. *et al.* The microbe-derived short chain fatty acid butyrate targets miRNA-dependent p21 gene expression in human colon cancer. *PLoS One* **6**, e16221 (2011).

41. Moloney, G. M., Viola, M. F., Hoban, A. E., Dinan, T. G. & Cryan, J. F. Faecal microRNAs: indicators of imbalance at the host-microbe interface? *Benef Microbes* **9**, 175–183 (2018).

42. Viennois, E. *et al.* Host-derived fecal microRNAs can indicate gut microbiota healthiness and ability to induce inflammation. *Theranostics* **9**, 4542–4557 (2019).

43. Lkhagva, E. *et al.* The regional diversity of gut microbiome along the GI tract of male C57BL/6 mice. *BMC Microbiol* **21**, 44 (2021).

44. Galley, J. D. *et al.* The structures of the colonic mucosa-associated and luminal microbial communities are distinct and differentially affected by a prolonged murine stressor. *Gut Microbes* **5**, 748–760 (2014).

45. Sun, S., Jones, R. B. & Fodor, A. A. Inference-based accuracy of metagenome prediction tools varies across sample types and functional categories. *Microbiome* **8**, 46 (2020).

46. Douglas, G. M. *et al.* PICRUSt2 for prediction of metagenome functions. *Nat Biotechnol* **38**, 685–688 (2020).

47. Lagkouvardos, I. *et al.* Sequence and cultivation study of Muribaculaceae reveals novel species, host preference, and functional potential of this yet undescribed family. *Microbiome* **7**, 28 (2019).

48. Bohacek, J., von Werdt, S. & Mansuy, I. M. Probing the germline-dependence of epigenetic inheritance using artificial insemination in mice. *Environ Epigenet* **2**, dvv015 (2016).

49. Park, H. J., Kim, S. A., Kang, W. S. & Kim, J. W. Early-life stress modulates gut microbiota and peripheral and central inflammation in a sex-dependent manner. *Int J Mol Sci* **22**, 1899 (2021).

50. Otaru, N. *et al.* GABA production by human intestinal *Bacteroides* spp.: prevalence, regulation, and role in acid stress tolerance. *Front Microbiol* **12**, (2021).

51. Constancias, F. & Mahé, F. fconstancias/metabaRpipe: v0.9 (v0.9). Zenodo. (2022) doi: 10.5281/zenodo.6423397.

52. Didion, J. P., Martin, M. & Collins, F. S. Atropos: specific, sensitive, and speedy trimming of sequencing reads. *PeerJ* **5**, e3720 (2017).

53. Callahan, B. J. *et al.* DADA2: High-resolution sample inference from Illumina amplicon data. *Nat Methods* **13**, 581–583 (2016).

54. R Core Team. R: A Language and Environment for Statistical Computing. R Foundation for Statistical Computing, Vienna, Austria (2022).

55. Oksanen, J. *et al.* vegan: community ecology package. https://CRAN.R-project.org/package=vegan (2020).

56. Paradis, E. & Schliep, K. ape 5.0: an environment for modern phylogenetics and evolutionary analyses in {R}. *Bioinformatics* **35**, 526–528 (2019).

57. Andersen, K. S., Kirkegaard, R. H., Karst, S. M. & Albertsen, M. ampvis2: an R package to analyse and visualise 16S rRNA amplicon data. *bioRxiv* (2018).

58. McLaren, M. speedyseq: faster implementations of phyloseq functions. https://github.com/mikemc/speedyseq (2021).

59. Mallick, H. *et al.* Multivariable association discovery in population-scale meta-omics studies. *PLoS Comput Biol* **17**, 1–27 (2021).

60. Constancias, F. & Sundar, S. fconstancias/DivComAnalyses: v0.9 (v0.9). Zenodo. (2022) doi:10.5281/zenodo.6473394.

61. Caspi, R. *et al.* The MetaCyc database of metabolic pathways and enzymes and the BioCyc collection of pathway/genome databases. *Nucleic Acids Res* **44**, D471–D480 (2016).

62. Wickham, H. *ggplot2: elegant graphics for data analysis*. (Springer-Verlag New York, 2016).

63. Gu, Z., Eils, R. & Schlesner, M. Complex heatmaps reveal patterns and correlations in multidimensional genomic data. *Bioinformatics* **32**, 2847–2849 (2016).

Data Availability

Raw sequences generated and analyzed during the current study are available in the European Nucleotide Archive repository under accession number PRJEB57336, https://www.ebi.ac.uk/ena/browser/view/PRJEB57336.

Acknowledgements

We thank Alfonso Die and Adam Krzystek for assistance with liquid chromatography analyzes. Illumina sequencing data were generated in collaboration with the Genetic Diversity Centre (GDC), ETH Zürich.

This work was supported by own resources (ETH Zürich and University Children's Hospital Zürich).

The Mansuy lab is funded by the University Zürich, the ETH Zürich, the Swiss National Science Foundation grant number 31003A_175742/1, the National Centre of Competence in Research (NCCR) RNA&Disease funded by the Swiss National Science Foundation (grant number 182880/Phase 2 and 205601/Phase 3), ETH grants (ETH-10 15-2 and ETH-17 13-2), European Union Horizon 2020 Research Innovation Program Grant number 848158, European Union projects FAMILY and HappyMums funded by the Swiss State Secretariat for Education, Research and Innovation (SERI), FreeNovation grant from Novartis Forschungsstiftung, and the Escher Family Fund.

Author contributions

CL, IM, CB, NO and BP designed the study. NO and LK performed the experiments. NO and FC performed the data analysis. CB, CL, and IM provided financial support. NO, BP, and CL drafted, and all authors critically reviewed the manuscript.

Competing interests

The authors declare that they have no competing interests.